

Calculating the hopping rate for diffusion in molecular liquids: CS₂

J. Daniel Gezelter, Eran Rabani, and B. J. Berne^{a)}

Department of Chemistry, Columbia University, 3000 Broadway, New York, New York 10027

(Received 16 October 1998; accepted 10 November 1998)

We extend the cage correlation function method for calculating the hopping rate in Zwanzig's model of self-diffusion in liquids [R. Zwanzig, *J. Chem. Phys.* **79**, 4507 (1983)] to liquids composed of polyatomic molecules. We find that the hopping rates defined by the cage correlation function drop to zero below the melting transition and we obtain excellent agreement with the diffusion constants calculated via the Einstein relation in liquids, solids, and supercooled liquids of CS₂. We also investigate the vibrational density of states of inherent structures in liquids which have rough potential energy surfaces, and conclude that the normal mode density of states at the local minima are not the correct vibrational frequencies for use in Zwanzig's model when it is applied to CS₂.

© 1999 American Institute of Physics. [S0021-9606(99)50507-2]

I. INTRODUCTION

In a recent series of papers,^{1,2} we have been investigating approaches to the calculation of hopping rates for Zwanzig's model of self-diffusion in liquids.³ This model has its roots in the inherent structure theory for liquids,⁴⁻⁷ and the primary result of the model is an expression for the diffusion constant,

$$D = \frac{kT}{M} \int_0^\infty d\omega \rho(\omega) \frac{\tau}{(1 + \omega^2 \tau^2)}, \quad (1)$$

in terms of the vibrational density of states in the inherent structures on the liquid's potential energy surface, $\rho(\omega)$, and a hopping time, τ , which characterizes the distribution [$\exp(-t/\tau)$] of residence times in the inherent structures. The primary quantity that must be obtained to make this model useful for a liquid is the hopping time τ . There are two approaches that have been presented in the literature for obtaining τ from simulations. The first approach attempts to calculate the hopping time from a static property—the fraction of imaginary frequency instantaneous normal modes.⁸⁻¹⁶ The other approach is to measure the decorrelation of atomic surroundings by associating the hopping rate ($1/\tau$) with the long-time decay rate of the cage correlation function.²

A. Instantaneous normal modes

Keyes and co-workers have approached the problem of obtaining the hopping time by using instantaneous normal modes (INMs).⁸⁻¹³ INMs are obtained by diagonalizing the matrix of second derivatives of the potential energy surface. Since the instantaneous configurations are not necessarily at the local minima, and since liquids contain anharmonicities, some of the INM frequencies will be imaginary. Averaging over many liquid configurations allows one to obtain a density of states of INM frequencies. The INM theory suggested by Keyes *et al.* interprets the fraction of imaginary frequency modes as an indicator of the number of barriers that are

accessible to the system, and indeed there is relatively good agreement between the fraction of unstable modes and the diffusion constant in some limited cases (i.e., liquids of moderate temperature). There have been other elaborations on the INM approach,¹⁴⁻¹⁸ which seek to correct some problems with the basic INM theory, but the underlying assumption that imaginary frequencies correlate with barrier crossings is the same.

In the most recent versions of the INM theory,^{15,16} one must first project the atomic coordinates along each of the instantaneous normal modes, and then classify the modes into three “flavors” according to the behavior of the potential energy surface along the projections. Those modes which have a double well (DW) in this projection are the ones that are assumed to be correlated with barrier crossings. Additionally, in computing the density of states of the DW modes, each mode is weighted by its projection onto center-of-mass translations of the molecules. The INM theory is then based on the assumption that the fraction of DW translational modes $f_{\text{DW}}^{\text{TR}}$ is correlated strongly with the diffusion constant.

We have previously argued against the INM approach because the imaginary frequency INMs (which may indeed measure anharmonicity on the potential energy surface) make up a substantial fraction of the modes in crystalline solids of Lennard-Jones atoms.¹ This system cannot cross any barriers to self-diffusion, so the imaginary frequency INMs contain many “false barriers.” The merits of the INM theory and our critique of it are still matters of intense debate.^{1,19-21} Interested readers should consult the original papers since the INM debate will not be the primary concern of this paper.

B. Cage correlation functions

In response to some of the problems that we observed with the INM approach, we developed the cage-correlation function.² The rate at which this function decays is a measure of the time it takes atoms to experience changes in their surroundings.

^{a)}Electronic mail: berne@chem.columbia.edu

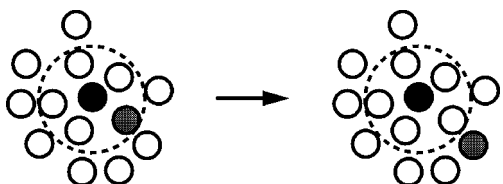


FIG. 1. A sketch of the idea behind the cage correlation function. The black atom's cage radius is denoted by the dotted line. The grey atom was inside the black atom's cage at time 0 (left side), but has exited the cage at time t (right side). The value of the cage correlation function is therefore 0 in the right figure even though four of the original five atoms stayed within the cage radius.

An atom's immediate surroundings are best described as those atoms immediately bonded to it, in addition to the other atoms in the liquid that make up the first solvation shell of the molecule. When a diffusive barrier crossing which involves the molecule has taken place, the atoms in the molecule have most likely left their immediate surroundings, and following the barrier crossing, they will have a slightly different group of atoms surrounding them. If one were able to paint identifying numbers on each of the atoms in a simulation, and kept track of the list of numbers that each atom could see at any time, then the barrier crossing event would be evident as a substantial change in this list of neighbors. This is precisely what is done when using neighbor lists in molecular dynamics simulations—where they are used to reduce the time spent on computing interatomic forces. Traditionally, the list of nearby atoms is updated every few time steps, and the forces are calculated using only those atoms that are within each atom's list of neighbors. This can save an immense amount of CPU time, and has become an invaluable technique in large simulations.²²

The cage correlation function uses a generalized neighbor list to keep track of each atom's neighbors. If the list of an atom's neighbors at time t is identical to the list of neighbors at time 0, the cage correlation function has a value of 1 for that atom. If any of the original neighbors are *missing* at time t , it is assumed that the atom participated in a hopping event and the cage correlation function is 0. This is shown graphically in Fig. 1.

Averaging over all atoms in the simulation, and studying the decay of the cage correlation function gives us a way to measure the hopping time directly from very short simulations.

We have previously investigated this function in Lennard-Jones systems,² and we now generalize the approach to molecular systems.

II. DIFFUSION OF POLYATOMIC MOLECULES

A generalized neighbor list (\mathcal{L}_i) for atom i in an N atom system is a vector of length N , and is defined as

$$\mathcal{L}_i \equiv \begin{pmatrix} f(r_{i1}) \\ \vdots \\ f(r_{iN}) \end{pmatrix}, \quad (2)$$

where $f(r_{ij})$ is a function of the interatomic distance (r_{ij}). In large simulations, $f(r_{ij})$ is typically taken as the Heaviside function,

$$f(r_{ij}) = \Theta(r_{\text{nlst}} - r_{ij}) = \begin{cases} 1 & \text{if } r_{ij} \leq r_{\text{nlst}} \\ 0 & \text{otherwise} \end{cases}, \quad (3)$$

where r_{nlst} is the neighbor list cutoff radius.

We have chosen r_{nlst} differently from how one would choose it to speed the calculation of forces. In calculating \mathcal{L}_i , we set r_{nlst} to the location of the minimum in the pair correlation function,²²

$$g(r) = \frac{V}{N^2} \left\langle \sum_i \sum_{j \neq i} \delta(\mathbf{r} - \mathbf{r}_{ij}) \right\rangle \quad (4)$$

that separates the first and second solvation shells. This distance is not necessarily the best choice for r_{nlst} , but it provides a starting point for the calculation of neighbor list correlation functions.

There are some quite striking properties of the correlation function,

$$C_{\mathcal{L}}(t) \equiv \frac{\langle \mathcal{L}_i(0) \cdot \mathcal{L}_i(t) \rangle}{\langle \mathcal{L}_i(0)^2 \rangle}, \quad (5)$$

for the radial cutoff neighbor lists. In our previous work,² we found that this function decays very slowly relative to other estimates of the hopping time τ . When an atom has been involved in a barrier crossing, many of the original members of that atom's neighbor list persist into the atom's new neighbor list. What we seek is a correlation function that is a measure of whether or not the cage has undergone *any* real change in time t . To compute this, we must first know the number of atoms that have left the neighbor list since the original configuration. The number of atoms that have left atom i 's original neighbor list at time t is

$$n_i^{\text{out}}(0, t) = |\mathcal{L}_i(0)|^2 - \mathcal{L}_i(0) \cdot \mathcal{L}_i(t). \quad (6)$$

In this equations, $|\mathcal{L}_i(t)|^2$ is the number of atoms in i 's neighbor list at time t , while $\mathcal{L}_i(0) \cdot \mathcal{L}_i(t)$ is the number of atoms that are in i 's neighbor list at both time 0 and time t .

Next we define c , which is the number of atoms that must leave an atom's neighbor list before we can be reasonably sure that a change in surroundings has taken place. The correlation function for the cage is then

$$C_{\text{cage}}^{\text{out}}(t) \equiv \langle \Theta(c - n_i^{\text{out}}(0, t)) \rangle. \quad (7)$$

(We have chosen $c = 1$ for the calculations in this paper.) A plot of a typical cage correlation function is shown in Fig. 2.

Since single atoms can leave and rejoin the neighbor list during normal vibrational motion, there is a significant decay of $C_{\text{cage}}(t)$ at short times. In liquids, there are two competing channels that contribute to the decay of the cage correlation function. In addition to the vibrational channel, the cage can change when the system has crossed a barrier on the potential energy surface. The phenomenological effect of the barrier crossing is a second decay of the cage correlation function that happens over much longer times.

The decay of correlation functions over multiple time scales is by no means a newly observed phenomenon. In the

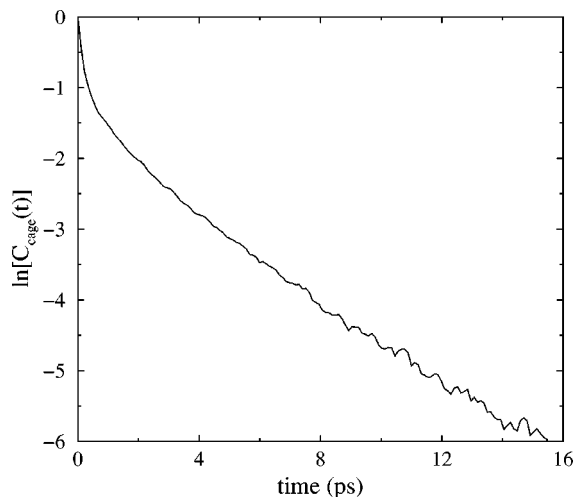


FIG. 2. A typical center-of-mass cage correlation function. This particular function is calculated for liquid CS₂ at a density of 1.46 g cm⁻³, a temperature of 242 K, and a cage radius of 5.2 Å. Note the fast initial (vibrational) decay at $t < 1$ ps and a slower exponential decay due to diffusional hopping for $t > 1$ ps.

late 1970's, Chandler, Montgomery, and Berne^{23,24} observed this phenomenon in the correlation function for fluctuations in the number of particles at the barrier to isomerization of a model double-well system. They treated the dynamics using the reactive flux method,²³⁻²⁶ which has often been used to study rare events in liquids.²⁷

In a molecular system like CS₂, there is a straightforward generalization of Eqs. (2)–(7). Instead of using the positions of the constituent atoms, one can instead replace atomic position with the centers-of-mass of the molecules themselves. To measure the hopping rate for spatial diffusion in CS₂, this is exactly what we have done. A typical center-of-mass cage correlation function for liquid CS₂ is shown in Fig. 2.

III. COMPUTATIONAL DETAILS

Simulations of liquid carbon disulphide were carried out using the intermolecular potential energy surface of Tildesley and Madden.²⁸ The form of the intermolecular potential between molecules i and j is a sum of pair interactions between sites on the two molecules,

$$V_{ij} = \sum_{\alpha=1}^3 \sum_{\beta=1}^3 V_{\alpha\beta}(r_{\alpha\beta}), \quad (8)$$

where the site–site potentials are given by

$$V_{\alpha\beta}(r_{\alpha\beta}) = 4\epsilon_{\alpha\beta} \left[\left(\frac{\sigma_{\alpha\beta}}{r_{\alpha\beta}} \right)^{12} - \left(\frac{\sigma_{\alpha\beta}}{r_{\alpha\beta}} \right)^6 \right], \quad (9)$$

and $\epsilon_{\alpha\beta}$ and $\sigma_{\alpha\beta}$ are the usual Lennard-Jones energy and length parameters. The cross terms (ϵ_{CS} and σ_{CS}) are taken from the traditional mixing rules for crossed interactions:

$$\sigma_{ab} = \frac{(\sigma_{aa} + \sigma_{bb})}{2}, \quad (10)$$

$$\epsilon_{ab} = \sqrt{\epsilon_{aa}\epsilon_{bb}}.$$

TABLE I. Parameters of the potential energy surface for liquid carbon disulphide.

Parameter	Value
σ_{CC}	3.35 Å
σ_{SS}	3.52 Å
ϵ_{CC}	0.1017 kcal mol ⁻¹
ϵ_{SS}	0.3637 kcal mol ⁻¹
θ_0	π rad
k_θ	85.15 kcal mol ⁻¹ rad ⁻²
D_0	167.38 kcal mol ⁻¹
b	1.82 Å ⁻¹
r_0	1.57 Å

In addition to the intermolecular potential, we have included terms for the intramolecular stretch and bends,

$$V_i = \frac{1}{2}k_\theta(\theta - \theta_0)^2 + D_0(1 - e^{-b(r_{12} - r_0)})^2 + D_0(1 - e^{-b(r_{23} - r_0)})^2, \quad (11)$$

with parameters chosen to match the vibrational frequencies for CS₂.²⁹ This form of the intramolecular potential was used by Moore and Keyes in their work on the instantaneous normal modes of liquid carbon disulphide.³⁰ The parameters (both inter- and intramolecular) are summarized in Table I.

All of our simulations were performed with 256 molecules in a constant-NVE ensemble. Trajectories of crystal-line CS₂ were started in the orthorhombic configuration (unit cell dimensions: $a = 6.379$ Å, $b = 5.566$ Å, $c = 8.973$ Å). Equilibration was assured by rescaling the velocities to match the target temperature for the system every 200 fs. Following a 50 ps period of equilibration, data were collected during uninterrupted runs of 100 ps in length. Configurations were saved every 500 fs from the data collection runs.

For the supercooled liquid trajectories, our quench programming started with a liquid at a density of $\rho = 1.46$ g cm⁻³ and a temperature of 280 K. After a 200 ps equilibration period, we quenched it to 260 K over 12 ps, with velocity rescalings performed every 100 fs. The trajectory was allowed to stabilize at the new temperature for 6 ps, and data were collected for 100 ps after the stabilization. The 12 ps quench, 6 ps stabilization, and 100 ps data collection process were repeated for temperatures at 20 K intervals down to 100 K.

The higher density ($\rho = 1.5875$ g cm⁻³) supercooled liquid trajectories were obtained in the same manner, but starting from an initial temperature of 400 K. The supercooled liquid trajectories utilized cubic box periodic boundary conditions to prevent crystallization.

The integrator used for the simulations was a reversible-RESPA integrator with the forces for the inner loop obtained from the intramolecular potential functions, while the forces for the outer loop came from the intermolecular potential.³¹ This integrator lets us run a trajectory $\sim 4\times$ faster than one which uses the standard velocity verlet integrator with forces computed using all atoms in the simulation. Minimum-image periodic boundary conditions were enforced using an orthorhombic box with the same length ratios as the unit cell in

the solid, but which had been scaled to give the correct density. The cutoff radius was chosen to be smaller than 1/2 of the length of the shortest of the simulation box dimensions.

Translational diffusion constants were computed from the stored trajectories using the standard Einstein relation:³²

$$D = \lim_{t \rightarrow \infty} \frac{1}{6t} \langle |\mathbf{r}_i(t) - \mathbf{r}_i(0)|^2 \rangle, \quad (12)$$

and were compared to the predictions of the Zwanzig model (using estimates of the hopping rate from both INM theory and from the cage correlation function).

Center-of-mass cage correlation functions are computed using a cage radius that is set to be the location in the second minimum in the pair correlation function [Eq. (4)]. Due to the anisotropy of the system around a single molecule of CS₂, the first solvation shell is split into two peaks in $g(r)$. Both peaks are included in that molecule's cage for the purposes of the cage correlation function calculation.

IV. RESULTS

A. Liquids and crystals

Using the hopping rates calculated from the decay of $C_{\text{cage}}(t)$, we can apply Zwanzig's model and calculate the self-diffusion constant. When the hopping time τ is very long, the rate ($k_h = 1/\tau$) is very small. If we rewrite Eq. (1) with this substitution,

$$D = \frac{k_B T}{M} \int_0^\infty d\omega \rho(\omega) \frac{k_h}{(k_h^2 + \omega^2)}, \quad (13)$$

then we can see that to a very good approximation, the rate can come outside of the integral, leaving

$$D \approx k_h \frac{k_B T}{M} \int_0^\infty d\omega \frac{\rho(\omega)}{\omega^2}. \quad (14)$$

To a good approximation, the integral is temperature independent, so the diffusion constant should scale linearly with the product of the temperature and hopping rate,

$$D \approx k_h \frac{k_B T}{M} g, \quad (15)$$

where g can be determined from integrating a known density of states, or by matching D to the experimentally determined diffusion constant at a single temperature. In the results presented below, we have used this approximation, and have determined g by matching the Einstein diffusion constant [Eq. (12)] to the right hand side of Eq. (15) at a temperature just above the melting transition. Our reasons for making this approximation are covered in greater detail in Sec. V. Results for liquids and crystalline solids at temperatures near the melting transition are shown in Figs. 3 and 4.

In contrast to the instantaneous normal mode theories,¹ the diffusion constants calculated via the cage correlation function are effectively zero for crystalline solids. Note that the data presented in Figs. 3 and 4 are obtained from con-

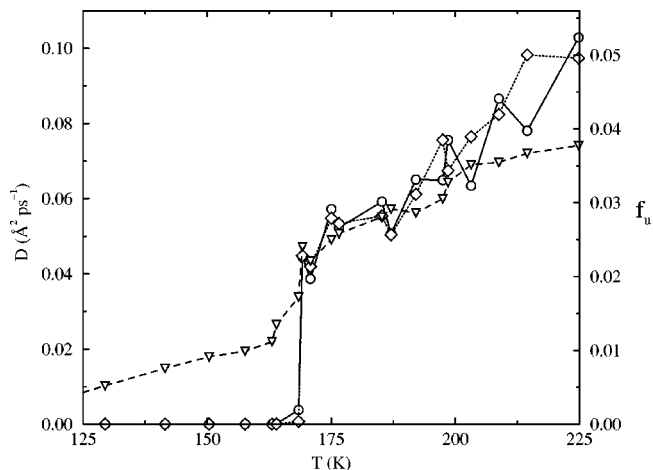


FIG. 3. Plots of the temperature dependence of the diffusion constant for equilibrium CS₂ near the melting transition for $\rho = 1.46 \text{ g cm}^{-3}$: (O) the diffusion constants calculated via the Einstein relation [Eq. (12)], and (\diamond) calculated via the center-of-mass cage correlation function [Eq. (7)] combined with the modified Zwanzig formula [Eq. (15)]. The fraction of unstable pure-translation instantaneous normal modes, f_u^{TR} is plotted (∇), and the scale for the fraction of unstable modes is along the left side of the figure.

stant energy trajectories, so the largest uncertainties are along the temperature axis. The data points each have a standard error of less than 5 K along this axis.

The present theory does quite well at predicting the translational diffusion constant in moderate and high density fluids for a wide range of temperatures. We know from our previous work,² and from the work of Mohanty³³ and Bagchi³⁴ that the hopping mechanism for self-diffusion in liquids breaks down when the hopping rate becomes too large. Therefore, the Zwanzig hopping model should be considered relevant only for moderate to high density liquids. The cage correlation function results begin to deviate from the Einstein relation when the hopping rate rises above 0.2 ps^{-1} , which is well into the liquid regime. We have two explanations for this deviation:

- (1) either the hopping mechanism begins to break down as the dominant mechanism for diffusion, or

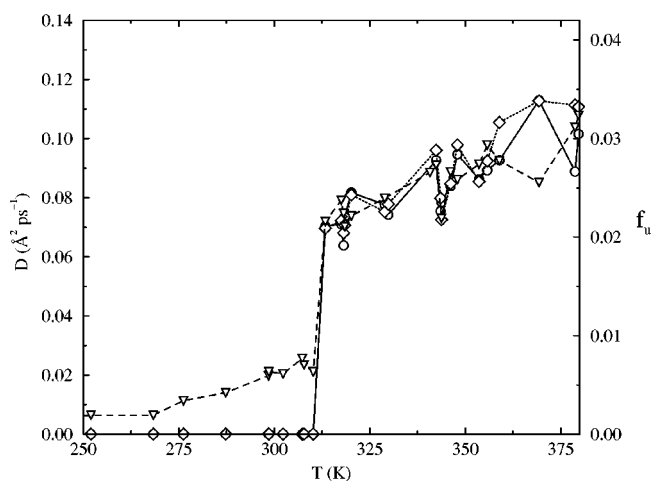


FIG. 4. The same as Fig. 3 but at a density of $\rho = 1.5875 \text{ g cm}^{-3}$.

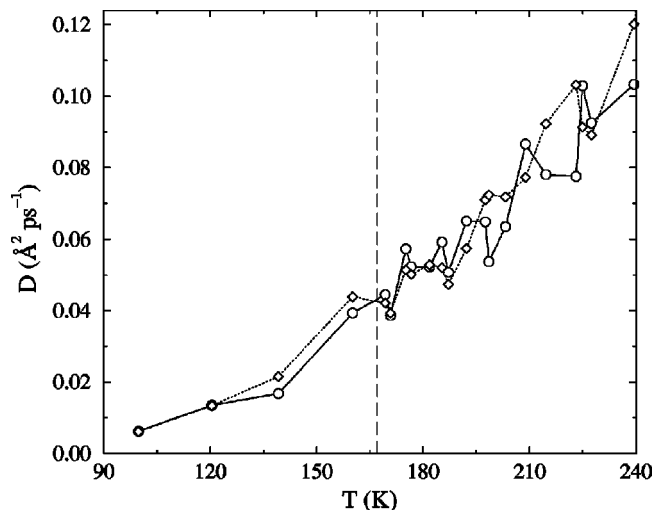


FIG. 5. The temperature dependence of the diffusion constant for regular and supercooled liquid CS_2 for $\rho = 1.46 \text{ g cm}^{-3}$: (○) diffusion constants calculated via the Einstein relation [Eq. (12)], and (◇) calculated via the center-of-mass cage correlation function [Eq. (7)] combined with the modified Zwanzig formula [Eq. (15)]. The temperature of the melting transition is shown by the vertical dashed line.

(2) the small rate approximation in Eq. (13) is invalid at higher temperatures.

A hopping model of diffusion is of greatest interest in physical systems (membranes, supercooled liquids and glasses) where the hopping rate is much smaller than the ceiling we report here, so methods based on the Zwanzig model are still of great utility.

B. Supercooled liquids

We have also calculated diffusion constants in the supercooled liquid regime using the center-of-mass cage correlation functions. We show comparisons of the current work to the Einstein diffusion constants in Figs. 5 and 6.

Note that as the temperature (and the diffusion and hopping rate) falls, the approximation in the modified Zwanzig formula [Eq. (15)] becomes more correct, so there is increasing agreement between the diffusion constants calculated via the cage correlation function and the results from the Einstein relation [Eq. (12)].

V. DISCUSSION

In Zwanzig's original work on an inherent structure model for diffusion, he used the Debye spectrum for the vibrational density of states.³ This was an approximation to the density of harmonic states in the liquid, and more recent elaborations on Zwanzig's model have attempted to provide more realistic vibrational densities of states around the liquid's inherent structures.

Keyes approximated the vibrational density of states with the functional form

$$\rho_{INM}(\omega) = (2\omega_s)^{-1} [1 - \cos(\pi\omega/\omega_s)], \quad (16)$$

where ω_s is taken from the maximum in the distribution of the stable branch of the instantaneous normal mode density of states.^{9,11}

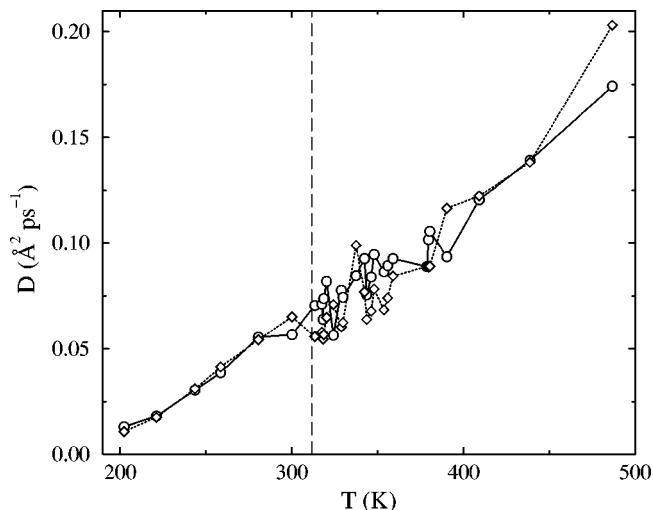


FIG. 6. The same as Fig. 5, but at a density of $\rho = 1.5875 \text{ g cm}^{-3}$.

A. The quenched density of states

Vijayadamodar and Nitzan have postulated that $\rho_q(\omega)$, the normal mode frequencies at the *quenched* configurations, should be used in Eq. (1).¹⁴ This idea builds on the inherent structure model since it associates the vibrational frequencies at the nearest local minima (the quenched configurations) with the vibrational frequencies of the liquid itself. In our original paper where we derived hopping rates from the cage-correlation function in a Lennard-Jones system,² we used the quenched density of states in Eq. (1) and obtained excellent agreement with the diffusion constant and with the velocity correlation function.

Given the success of using the quenched density of states for atomic liquids, we were surprised to find that the same density of states does not work in liquid CS_2 . (We assume here that the cage correlation function gives an accurate measure of the hopping times in this liquid – a reasonable assumption given the accuracy of this method in Lennard-Jones systems.) To compute the pure-translation density of states¹⁵ $\rho_q^{\text{TR}}(\omega)$ for CS_2 we constructed Hessians, which consisted of the second derivatives of the potential energy surface with respect to the (mass-weighted) coordinates of the molecular centers-of-mass:

$$K_{ix,jx'} = M \left(\frac{\partial^2 V}{\partial q_{ix} \partial q_{jx'}} \right), \quad (17)$$

where the center-of-mass coordinates are obtained trivially from the atomic coordinates

$$q_{ix} = \sum_{\alpha=1}^3 \frac{m_{\alpha} q_{i\alpha}}{M}. \quad (18)$$

The Hessian is then diagonalized (for a number of quenched configurations) to give the normal mode vibrational frequencies, and these frequencies are used to construct the translational density of states.

The *low*-frequency behavior of $\rho(\omega)$ is most important for accurate estimates of the diffusion coefficient [cf. Eqs. (13) and (14) which weight the low frequency part of the

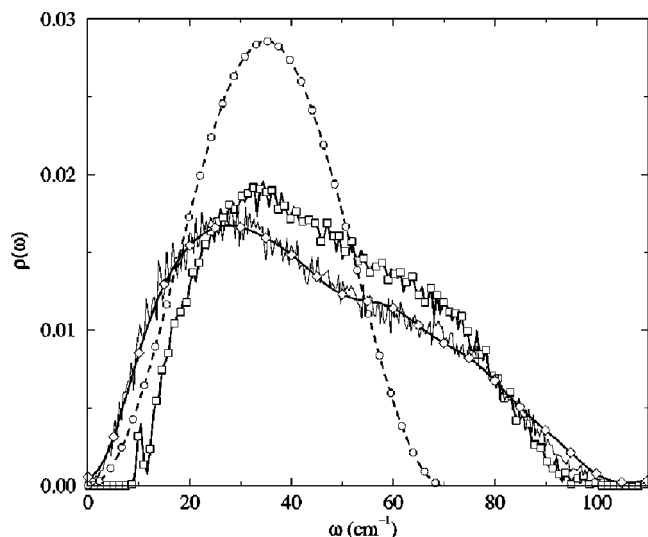


FIG. 7. The different candidates for the vibrational density of states for liquid CS_2 at a density of 1.46 g cm^{-3} : (\square) from the quenched configurations [$\rho_q(\omega)$], (\circ) obtained from Eq. (16), (\diamond) are $\rho^{(0)}(\omega)$, and the thin solid line is $\rho_q^{(0)}(\omega)$.

spectrum by $1/\omega^2$]. The observed quenched density of states (see Fig. 7) displays a low-frequency ($0\text{--}10 \text{ cm}^{-1}$) gap and thus predicts a diffusion coefficient much smaller than the correct one. It is easy to understand why a low-frequency gap should occur in systems with very rough energy landscapes. From the schematic given in Fig. 8 we note that the system quenches into local minima with high frequencies—thus the gap. For such systems it would be a mistake to use the quenched density of states in the Zwanzig theory.

It would seem then that the vibrations which are most relevant to Zwanzig's model are those that involve the system as it moves from one end of a large basin to another (i.e., from one diffusive barrier to another). The normal mode frequencies in each of the individual local minima may have little relation to frequencies of the basin vibrations. (An extreme form of this would be the hard-sphere liquid, for which there are no vibrational frequencies at the quenched configurations.)

In atomic Lennard-Jones systems, the quenched density of states appears to mimic the density of states of these large-scale "basin" vibrations.² This indicates to us that there is very little roughness on the atomic liquid's potential energy surface. One possible explanation for this is that the Lennard-Jones potential energy surface has only one well depth while the CS_2 surface has three different wells (S–S, C–C, and C–S). Slight deviations in molecular orientations can therefore lead to small barriers between nearby local minima.

B. Estimating $\rho(\omega)$ from power spectra

The spirit of the Zwanzig model is to recognize that the velocity autocorrelation function $C(t) = \langle \mathbf{v}(t) \cdot \mathbf{v}(0) \rangle$ decays due to hopping over diffusive barriers in addition to the decay from vibrational motion that occurs inside the basin. If we define a zeroth-order velocity autocorrelation function [$C^{(0)}(t)$] for those trajectories which remain in the initial

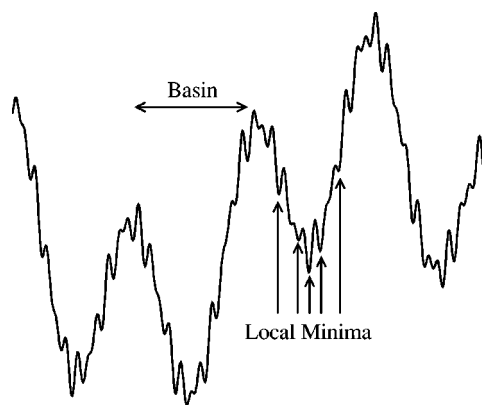


FIG. 8. A sketch of a "rough" potential energy surface which has a distribution of small barriers superimposed on the real barriers to diffusion which separate the basins from one another.

basin, then the overall correlation function is a product of the zeroth-order part and the survival probability in the basins, which is taken to be exponential:

$$C(t) = C^{(0)}(t) e^{-t/\tau}, \quad (19)$$

since (within the Zwanzig model) hopping over the barrier will destroy any correlations that may exist prior to the hop.

The decay of $C^{(0)}(t)$ can be understood simply as the loss of correlation due to vibrational motion within a basin,

$$C^{(0)}(t) = \int_0^\infty d\omega \rho^{(0)}(\omega) \cos(\omega t), \quad (20)$$

where $\rho^{(0)}(\omega)$ is the power spectrum of $C^{(0)}(t)$, which we call the density of vibrational states in the basin. In the original Zwanzig formulation, the motion is assumed to be harmonic. We stress that $\rho^{(0)}(\omega)$ is *not* identical to the power spectrum of the full velocity autocorrelation function, but is the power spectrum for those trajectories which do not hop over diffusive barriers.

Zwanzig's model writes the full velocity autocorrelation function in terms of the vibrational modes in the basins and then uses the Green–Kubo relation to extract the diffusion constant [cf. Eq. (1)]. Since we already have a method for obtaining the hopping time τ , we can attempt to extract the density of states in the basin by following the logic of the Zwanzig model. We simply write the correlation function in terms of the basin modes [$\rho^{(0)}(\omega)$],

$$C(t) = \int_0^\infty d\omega \rho^{(0)}(\omega) \cos(\omega t) e^{-t/\tau}, \quad (21)$$

and then use a singular value decomposition (SVD)³⁵ to back out a discrete representation of $\rho^{(0)}(\omega)$ from values for the velocity autocorrelation function determined from molecular dynamics. Note that we are simply finding the $\rho^{(0)}(\omega)$ that gives the best fit to the velocity autocorrelation function at a single temperature. The density of states $\rho^{(0)}(\omega)$, so obtained (and shown in Fig. 7), does not display a gap as does the quenched density of states. Interestingly, when we determined $\rho^{(0)}(\omega)$ for a wide range of temperatures from a SVD analysis of Eq. (21) using the values of τ at the different temperatures we obtained from the cage correlation function,

we found that $\rho^{(0)}(\omega)$ is not sensitive to the temperature. Our observed $\rho^{(0)}(\omega)$ (calculated at a temperature of 280 K) is displayed in Fig. 7.

Thus $\rho^{(0)}(\omega)$ need only be determined at one temperature for each liquid density. This information together with the Green–Kubo relation for the translational diffusion coefficient, using Eqs. (20) and (21), allows determination of D ,

$$D = \frac{k_B T}{M} \int_0^\infty d\omega \rho^{(0)}(\omega) \frac{\tau}{\omega^2 \tau^2 + 1}. \quad (22)$$

If $\rho^{(0)}(\omega)$ is really the density of states for motion in a basin, we should be able to observe it as the power spectrum of $C(t)$ for trajectories which *do not* hop over the large diffusive barriers. Given the observations that: (a) the quenched density of states $\rho_q(\omega)$ has a frequency gap but $\rho^{(0)}(\omega)$ does not, and (b) $\rho^{(0)}(\omega)$ appears to be independent of temperature, we have tried the following experiment: We computed velocity correlation functions for an ensemble of trajectories that was generated by starting at the quenched configurations, giving each configuration just enough thermal energy (~ 5 K) so that they were not able to cross the large diffusive barriers. Fourier transforming these velocity correlation functions enabled us to extract the density of states easily from short low-temperature simulations. This average density of states, which we call $\rho_q^{(0)}(\omega)$, is also plotted in Fig. 7.

As expected, we see that $\rho^{(0)}(\omega)$ and $\rho_q^{(0)}(\omega)$ are very similar (except at very low frequencies where the SVD approach is slightly larger), and both are quite different from the quenched density of states. $\rho^{(0)}(\omega)$ and $\rho_q^{(0)}(\omega)$ both contain more low-frequency vibrations than we have observed in the quenched density of states, so even the small amount of thermal motion in the system at 5 K recovers the low-frequency motions related to anharmonicity. (Similar experiments at 10 and 15 K show similar results, so we expect that $\rho_q^{(0)}(\omega)$ is also independent of temperature.)

We do not mean to suggest that either of these two approaches [calculating $\rho^{(0)}(\omega)$ or $\rho_q^{(0)}(\omega)$] are good ways of calculating diffusion constants or testing the Zwanzig model. (The SVD approach is circular in that it assumes that both the Zwanzig model and a particular method of computing hopping times are correct.) Indeed, when these two methods are used to calculate diffusion constants in Eq. (1) the diffusion constants differ from each other by almost a factor of 2. Since the two densities of states are so similar except for the very lowest frequencies ($< 1 \text{ cm}^{-1}$), this suggests that Eq. (1) is *extremely* sensitive to the lowest part of the frequency range. One can make very small errors in the lowest frequencies (i.e., within the error bars for the density of states) which result in very large changes in the diffusion constants.

What these investigations do tell us is that one would need exceedingly accurate estimates of the density of states at the very lowest frequencies to compute diffusion constants using Eq. (1) when the potential energy surface is rough.

Table II compares the errors one obtains in diffusion constants using the above estimates for $\rho(\omega)$.

TABLE II. Relative errors, $\langle (D_{\text{predicted}} - D)/D \rangle$ in the self-diffusion constants computed using Eq. (1) and the four proposed methods for obtaining the vibrational density of states. Results for two different liquid densities are shown.

Method for estimating $\rho(\omega)$	% error in D	
	Liquid density	
	1.46 g cm ⁻³	1.5875 g cm ⁻³
$\rho_q(\omega)$	-88%	-88%
$\rho_{INM}(\omega)$ (Eq. (16))	-75%	-80%
$\rho^{(0)}(\omega)$	+11%	-23%
$\rho_q^{(0)}(\omega)$	-63%	-55%

C. Computational cost

If one wishes to calculate diffusion coefficients in high-temperature liquids, the traditional method of using the mean square displacement [Eq. (12)] is usually quite efficient. However, at lower temperatures and in the supercooled regime, the simulation time required to converge the slope of the mean square displacement becomes prohibitive. The Zwanzig hopping model allows one to avoid these long simulations if the characteristic time of residence between hops is short relative to the convergence time for the slope of the mean square displacement. In Sec. III, we have given details of an efficient way of obtaining the hopping time from short simulations, and now the issue of computational cost rests on estimating the density of states in the liquid.

The simplest approach to this estimate is to avoid it altogether by making the small rate approximation. One simply computes the diffusion coefficient using mean square displacements at a relatively high temperature (where the standard approach is not computationally prohibitive), and then uses this diffusion coefficient to scale the results from the hopping times as in Eq. (15). The slow step in this method is the calculation of the mean square displacement at the high temperature, which does require a fairly long simulation, but needs to be done only once for each liquid density.

Using the quenched density of states $\rho_q(\omega)$ requires the collection of quenched configurations (local minima) by steepest descent from a set of statistically independent liquid configurations. This can be very time consuming, particularly when the liquid contains a mixture of high- and low-frequency vibrational degrees of freedom (as is the case in CS₂). Obtaining the normal mode frequencies at these configurations is simply a matter of diagonalizing the mass-weighted Hessian, which rises in computational cost with the cube of the number of molecules in the simulation. More importantly, the quenched density of states does not give good diffusion coefficients.

Slightly cheaper than the quenched density of states is the calculation of $\rho_q^{(0)}(\omega)$ via a Fourier transform of short-time trajectories carried out at ~ 5 K above the quenched configurations. The short trajectories and the Fourier transforms are both inexpensive, but one must still start from the quenched configurations, and obtaining these can be expensive.

The cheapest method of obtaining an estimate of the density of states is the calculation of $\rho^{(0)}(\omega)$ via SVD of the velocity autocorrelation function at a temperature for which the hopping time is known. The SVD procedure that produced $\rho^{(0)}(\omega)$ in Fig. 7 involved a 2000×2000 matrix diagonalization, but since $\rho^{(0)}(\omega)$ is largely independent of temperature, this is done only once for each liquid density.

D. Summary

We now know that neither $\rho_q(\omega)$ nor $\rho_{INM}(\omega)$ gives a good estimate of the density of states in this liquid. However, we do not know which of the power-spectrum methods for estimating it is “correct.” We can make plausible arguments for both of them, and since they result in different vibrational densities of states, they give rise to different diffusion constants in Zwanzig’s model. As stated at the beginning of Sec. IV, we have used the small rate approximation to calculate diffusion constants in CS₂, matching the constant g in Eq. (15) to obtain agreement just above melting. It is not satisfying to leave a free parameter in the theory, but without an accurate means of obtaining the vibrational density of states for a liquid, and in systems for which the hopping rate is small, this is a reasonable approach. It would therefore be of great interest to have a method for estimating the true vibrational density of states (particularly at the lowest frequencies) on a rough potential energy surface.

VI. CONCLUSION

In the preceding sections, we have extended to molecular liquids a method for using molecular dynamics simulations to estimate the hopping rate for the Zwanzig model of self-diffusion [Eq. (1)]. We associate the hopping rate with the slow decay of the cage correlation function [Eq. (7)], where the cage radius is measured from the center of mass of each of the molecules in the liquid, and membership in a molecule’s cage is determined by comparing center-of-mass distances for the other molecules in the liquid. We associate the fast initial decay of the cage correlation function either with simple vibrational and librational motion of the liquid, or with barrier crossings of the small perturbing barriers on a rough potential energy surface—barriers which are not the barriers to diffusion.

Because the hopping rate in this system is relatively small, we have been able to make a simplification to the Zwanzig model, and have seen excellent agreement between the self-diffusion constants calculated with our method and those calculated via the Einstein relation [Eq. (12)], particularly in the supercooled liquid regime, where convergence of the Einstein relation is very slow. Since our method requires simulations that are just long enough to observe the slow decay of the cage correlation function (~ 10 ps for the lowest temperatures studied), and since the Einstein relation requires 50–100 ps for convergence in the same system, our method results in substantial savings in CPU time.

We therefore repeat an important caveat for use of the Zwanzig model (in any form) for systems with rough potential energy surfaces. The original formulation of the Zwanzig model utilized the density of states of the “inherent struc-

tures” of the liquid. This has usually been taken to mean the normal mode density of states at the nearest local minimum on the potential energy surface. This works quite well in atomic Lennard-Jones systems, which have relatively simple potential energy surfaces. We now know that when the potential energy surface is rough (as in CS₂) these vibrational frequencies can be quite different from those the liquid experiences when it can traverse the small nondiffusive barriers. Our evidence for this is shown quite graphically in Fig. 7 where the normal mode density of states is missing the important low-frequency modes that are present when one observes vibrational frequencies from a supercooled liquid at nonzero temperature. If one were to apply the Zwanzig model to this system naively [i.e., using $\rho_q(\omega)$ in Eq. (1)] there would be substantial errors in the predicted diffusion constants.

Although we can eliminate some methods of estimating $\rho(\omega)$ from consideration, we do not yet have a satisfying way of arriving at a density of states for the basins on a rough potential energy surface, so there is still a free parameter in the current method for determining the diffusion constant. Even with this caveat, the cage correlation function provides an efficient way to measure the hopping time for diffusive motion, and gives excellent agreement with the diffusion constants obtained with more computationally expensive methods.

We must also entertain the possibility that a model built on interrupted basin vibrations in what is an essentially anharmonic system will not be able to predict diffusion accurately. Alternative hopping models (like the one proposed by Hartmann and Heermann)³⁶ which accumulate hopping distances as well as hopping times may be more useful in some systems where the Zwanzig model breaks down.

ACKNOWLEDGMENTS

E.R. is a Rothschild and Fulbright postdoctoral fellow. This work was supported by a grant to B.J.B. from the National Science Foundation.

- ¹J. D. Gezelter, E. Rabani, and B. J. Berne, *J. Chem. Phys.* **107**, 4618 (1997).
- ²E. Rabani, J. D. Gezelter, and B. J. Berne, *J. Chem. Phys.* **107**, 6867 (1997).
- ³R. Zwanzig, *J. Chem. Phys.* **79**, 4507 (1983).
- ⁴F. H. Stillinger and T. A. Weber, *Phys. Rev. A* **25**, 978 (1982).
- ⁵F. H. Stillinger and T. A. Weber, *Phys. Rev. A* **28**, 2408 (1983).
- ⁶T. A. Weber and F. H. Stillinger, *J. Chem. Phys.* **80**, 2742 (1984).
- ⁷F. H. Stillinger and T. A. Weber, *J. Chem. Phys.* **83**, 4767 (1985).
- ⁸G. Seeley and T. Keyes, *J. Chem. Phys.* **91**, 5581 (1989).
- ⁹B. Madan, T. Keyes, and G. Seeley, *J. Chem. Phys.* **92**, 7565 (1990).
- ¹⁰G. Seeley, T. Keyes, and B. Madan, *J. Chem. Phys.* **95**, 3847 (1991).
- ¹¹T. Keyes, *J. Chem. Phys.* **101**, 5081 (1994).
- ¹²T. Keyes, *J. Chem. Phys.* **104**, 9349 (1996).
- ¹³T. Keyes, *J. Chem. Phys.* **106**, 46 (1997).
- ¹⁴G. V. Vijayadmodar and A. Nitzan, *J. Chem. Phys.* **103**, 2169 (1995).
- ¹⁵W.-X. Li and T. Keyes, *J. Chem. Phys.* **107**, 7275 (1997).
- ¹⁶W.-X. Li, T. Keyes, and F. Sciortino, *J. Chem. Phys.* **108**, 252 (1998).
- ¹⁷S. D. Bembenek and B. B. Laird, *Phys. Rev. Lett.* **74**, 936 (1995).
- ¹⁸S. D. Bembenek and B. B. Laird, *J. Chem. Phys.* **104**, 5199 (1996).
- ¹⁹M. C. C. Ribeiro and P. A. Madden, *J. Chem. Phys.* **108**, 3256 (1998).
- ²⁰T. Keyes, W.-X. Li, and U. Zürcher, *J. Chem. Phys.* **109**, 4693 (1998).
- ²¹J. D. Gezelter, E. Rabani, and B. J. Berne, *J. Chem. Phys.* **109**, 4695 (1998).

- ²²M. P. Allen and D. J. Tildesley, *Computer Simulation of Liquids* (Oxford University Press, Oxford, 1987).
- ²³D. Chandler, *J. Chem. Phys.* **68**, 2959 (1978).
- ²⁴J. A. Montgomery, Jr., D. Chandler, and B. J. Berne, *J. Chem. Phys.* **70**, 4056 (1979).
- ²⁵J. B. Anderson, *J. Chem. Phys.* **58**, 4684 (1973).
- ²⁶C. H. Bennett, in *Algorithms for Chemical Computations*, edited by R. E. Christofferson (American Chemical Society, Washington D. C., 1977), p. 63.
- ²⁷B. J. Berne, in *Multiple Time Scales*, edited by J. U. Brackbill and B. I. Cohen (Academic, New York, 1995), pp. 419–436.
- ²⁸D. J. Tildesley and P. A. Madden, *Mol. Phys.* **42**, 1157 (1981).
- ²⁹G. Herzberg, *Molecular Spectra and Molecular Structure*, Infrared and Raman Spectra of Polyatomic Molecules Vol. II (Van Nostrand, Princeton, NJ, 1945).
- ³⁰P. Moore and T. Keyes, *J. Chem. Phys.* **100**, 6709 (1994).
- ³¹M. Tuckerman, B. J. Berne, and G. J. Martyna, *J. Chem. Phys.* **97**, 1990 (1992).
- ³²B. J. Berne and R. Pecora, *Dynamic Light Scattering* (Krieger, Malabar, FL, 1990).
- ³³U. Mohanty, *Phys. Rev. A* **32**, 3055 (1985).
- ³⁴B. Bagchi, *J. Chem. Phys.* **101**, 9946 (1994).
- ³⁵W. H. Press, S. A. Teukolsky, W. T. Vetterling, and B. P. Flannery, *Numerical Recipes in C* (Cambridge University Press, New York, 1992), Chap. 2.
- ³⁶A. K. Hartmann and D. W. Heermann, *J. Chem. Phys.* **108**, 9550 (1998).